International Journal of Solids and Structures 50 (2013) 519–530

Contents lists available at SciVerse ScienceDirect

International Journal of Solids and Structures

journal homepage: www.elsevier.com/locate/ijsolstr

Mechanical behavior of sandwich composite beams made of foams and functionally graded materials

M. Bîrsan [a,b,*], T. Sadowski [b], L. Marsavina [c], E. Linul [c], D. Pietras [b]

[a] Department of Mathematics, University "A.I. Cuza" of Iaşi, 700506 Iaşi, Romania
[b] Faculty of Civil Engineering and Architecture, Lublin University of Technology, Poland
[c] Department Strength of Materials, Politehnica University of Timişoara, Romania

ARTICLE INFO

Article history:
Received 15 October 2011
Received in revised form 8 April 2012
Available online 2 November 2012

Keywords:
Composite materials
Foam structures
Functionally graded
Sandwich materials
Effective stiffness properties
Beam
Bending

ABSTRACT

We investigate sandwich composite beams using a direct approach which models slender bodies as deformable curves endowed with a certain microstructure. We derive general formulas for the effective stiffness coefficients of composite elastic beams made of several non-homogeneous materials. A special attention is given to sandwich beams with foam core, which are made of functionally graded or piecewise homogeneous materials. In the case of small deformations, the theoretical predictions are compared with experimental measurements for the three-point bending of sandwich beams, showing a very good agreement. For functionally graded sandwich columns we obtain the analytical solutions of bending, torsion and extension problems and compare them with numerical results computed by the finite element method.

© 2012 Elsevier Ltd. All rights reserved.

1. Introduction

The mechanical behavior of composite beams is a topic of continued and increasing interest because this kind of slender structures are widely used in engineering devices. The emergence of new advanced materials, such as functionally graded foams, has given a new impulse to the research studies in this field.

In our work we employ a Cosserat-type approach for rod-like bodies to investigate the mechanical behavior of composite elastic beams. In this approach, also called the theory of directed curves, the slender body is represented as a deformable curve endowed with a triad of rigidly rotating unit vectors (also called directors) attached to each point. The motion of these triads of directors accounts for rotations of the cross-sections about the middle axis of the beam.

The theory of directed curves has been presented by Zhilin (2006, 2007). An extension of this model for porous and thermoelastic rods has been recently established by Bîrsan and Altenbach (2011a,b). We mention that the approach of directed curves is related to the so-called Cosserat theory for rods, which uses a set of deformable directors attached to the curve, see e.g. Green and Naghdi (1979), Rubin (2000). If one imposes certain constraints on the set of directors, then the theory of directed curves can be regarded as a special case of the nonlinear theory proposed by Antman (1972, 1995), Simo (1985). These latter theories are special cases of the nonlinear theory proposed by Green et al. (1979). In Section 2 we briefly present the kinematical model, the equilibrium equations, and the structure of constitutive equations for composite elastic rods, using the direct approach.

The main goal of this paper is to determine the analytical expressions of the effective stiffness coefficients for various types of composite beams, in terms of the three-dimensional parameters of the thin structure. To determine the effective stiffness coefficients, we compare the analytical solutions of bending, torsion, and extension problems for directed curves with the corresponding results for three-dimensional rods. This general procedure for non-homogeneous beams is described in Section 3. In Section 4 we generalize the results to the case of composite beams made of several different non-homogeneous materials. We present general formulas for the effective stiffness coefficients, which are expressed in terms of the solutions to some boundary-value problems formulated on the cross-section domain. These formulas (namely the relations (29), (30)) are applicable for a large variety of situations, including sandwich beams made of functionally graded materials and foams. Another type of important structures are the metal-ceramic composites. The mechanical response of polycrystalline ceramics containing metallic intergranular layers has been investigated in Sadowski et al. (2005, 2006), Postek and Sadowski (2011). In the next sections we illustrate the usefulness of our formulas by considering different types of sandwich beams.

* Corresponding author at: Department of Mathematics, University "A.I. Cuza" of Iaşi, 700506 Iaşi, Romania. Tel.: +40 232 201226; fax: +40 232201160.
E-mail address: bmircea@uaic.ro (M. Bîrsan).

0020-7683/$ - see front matter © 2012 Elsevier Ltd. All rights reserved.
http://dx.doi.org/10.1016/j.ijsolstr.2012.10.011

Sandwich structures are widely used because of their ability to provide high bending moment stiffness coupled with light weight. Because of this, sandwich panels are often used in applications where weight saving is critical: in aviation, ship building and construction (Zenkert, 1995). In most applications the sandwich panel must have some required minimum stiffness, it must not fail under some in service loading and it must be as light as possible. Its design can be formulated as an optimization problem: the goal is the panel with minimum weight which meets the requirements for stiffness and strength. For this purpose it is very important to used accurate solutions in order to estimate the stiffness of such structures.

In Section 5 we focus our attention to sandwich beams with foam core and determine the analytical expressions for effective bending stiffness, shear stiffness, and torsional rigidity. We compare our results with the classical expressions taken from Allen (1969), Zenkert (1997), Gibson and Ashby (1997), Timoshenko and Goodier (1951). Moreover, we verify the (new and classical) theoretical results by comparison with experimental measurements obtained for the three-point bending of sandwich beams. In Section 6 we extend our analysis to sandwich beams with dissimilar faces.

Section 7 is concerned with circular sandwich columns. For functionally graded sandwich columns obeying an exponential law of material distribution, we find the effective bending, shear, extensional, and torsion stiffness coefficients. Then, we compare these theoretical results with numerical solutions for some elastostatic problems solved by the finite element method.

The good agreement between the analytical, experimental, and numerical results shows that the proposed formulas for effective stiffness coefficients are correct, and they can be successfully used in applications.

2. Theoretical background

Let us present briefly the kinematical model of directed rods, which is described in details in Zhilin (2006, 2007), Bîrsan and Altenbach (2011a). Let $\mathcal{C}_0$ be the reference (initial) configuration of the deformable curve, and denote by s the material coordinate along $\mathcal{C}_0$, which is chosen to be the arclength parameter. The configuration is determined by the position vector $\boldsymbol{r}(s)$ and the attached directors $\boldsymbol{d}_i(s),\ i=1,2,3$. We take $\boldsymbol{d}_i(s)$ to be 3 orthogonal unit vectors, such that $\boldsymbol{d}_3(s)$ coincides with the unit tangent $\boldsymbol{t}\equiv\boldsymbol{r}'(s)$ (see Fig. 1). The vectors $\boldsymbol{d}_1$ and $\boldsymbol{d}_2$ belong to the normal plane to the curve $\mathcal{C}_0$ and they are usually chosen along the principal axes of inertia of the cross-section.

In the deformed configuration $\mathcal{C}$ at time $t$the position vector is denoted by $\boldsymbol{R}=\boldsymbol{R}(s,t)$, and the 3 directors are $\boldsymbol{D}_i=\boldsymbol{D}_i(s,t)$. The vector $\boldsymbol{D}_3$ is no longer tangent to the curve $\mathcal{C}$, since the initial cross-sections are not necessarily normal to the middle curve after deformation. Thus, the model allows for transverse shear deformation of the rod. On the other hand, the deformation of the cross-sections is not taken into account, which is a reasonable assumption for thin rods.

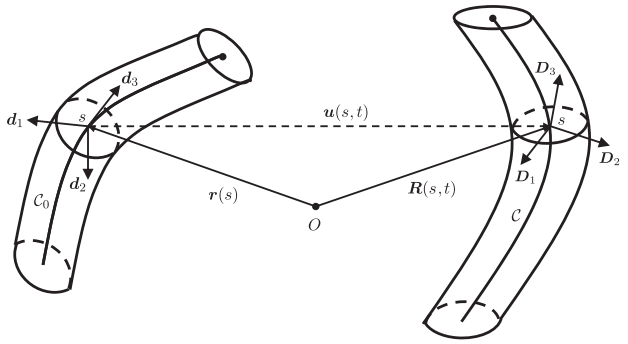

Fig. 1. The reference configuration $\mathcal{C}_0$ and the deformed configuration $\mathcal{C}$ of the directed curve.

Throughout the paper we employ the Einstein's summation convention and the direct tensor notation in the sense of Lurie (2005). Greek indices range over the set $\{1,2\}$, while Latin indices take the values $\{1,2,3\}$. We denote the material time derivative by a superposed dot and the derivative with respect to the spatial coordinate s by $()'=\frac{\mathrm{d}}{\mathrm{d}s}$.

With these notations, the rotation tensor is given by $\boldsymbol{P}(s,t)=\boldsymbol{D}_k(s,t)\otimes\boldsymbol{d}_k(s)$. In the linear theory of rods, the displacement vector $\boldsymbol{u}(s,t)=\boldsymbol{R}(s,t)-\boldsymbol{r}(s)$ is small. The rotation tensor can be represented as $\boldsymbol{P}=\boldsymbol{1}+\boldsymbol{\psi}\times\boldsymbol{1}$, where $\boldsymbol{\psi}(s,t)$ is the vector of small rotations. In the case of small strains, the deformation of the rod is characterized by the vector of extension-shear $\boldsymbol{e}$ and the vector of bending-twisting $\boldsymbol{\kappa}$, which are given by

$$\boldsymbol{e}=\boldsymbol{u}'+\boldsymbol{t}\times\boldsymbol{\psi},\qquad \boldsymbol{\kappa}=\boldsymbol{\psi}'. \tag{1}$$

Remark. In order to explain the definition of the extension-shear vector $\boldsymbol{e}$, let us consider the three-dimensional rod, with the position vector of a generic point in the reference configuration given by

$$\boldsymbol{r}^*(s,x_1,x_2)=\boldsymbol{r}(s)+x_1\boldsymbol{d}_1(s)+x_2\boldsymbol{d}_2(s), \tag{2}$$

where $(x_1,x_2)\in\Sigma$ are the material coordinates in the cross-section, and Σ is a given domain. After deformation, the material point will have the position vector

$$\boldsymbol{R}^*(s,x_1,x_2,t)=\boldsymbol{R}(s,t)+x_1\boldsymbol{D}_1(s,t)+x_2\boldsymbol{D}_2(s,t). \tag{3}$$

Then, the components ε_{ij} of the Lagrangian strain are given by

$$\begin{aligned}&\varepsilon_{\alpha\beta}=\frac{1}{2}(\boldsymbol{D}_\alpha\cdot\boldsymbol{D}_\beta-\delta_{\alpha\beta})=0,\quad \varepsilon_{\alpha3}=\frac{1}{2}(\boldsymbol{D}_\alpha\cdot\boldsymbol{R}'),\\ &\varepsilon_{33}=\frac{1}{2}(\boldsymbol{R}'\cdot\boldsymbol{R}'-1),\end{aligned} \tag{4}$$

at the centerline. On the other hand, in view of the relations $(1)_1$ and $\boldsymbol{D}_k=\boldsymbol{d}_k+\boldsymbol{\psi}\times\boldsymbol{d}_k, \boldsymbol{R}'=\boldsymbol{t}+\boldsymbol{u}'$, we deduce that (in the approximation of linear theory)

$$\boldsymbol{e}\cdot\boldsymbol{d}_\alpha=\boldsymbol{D}_\alpha\cdot\boldsymbol{R}',\quad \boldsymbol{e}\cdot\boldsymbol{t}=\frac{1}{2}(\boldsymbol{R}'\cdot\boldsymbol{R}'-1). \tag{5}$$

From (4) and (5) we see that the cross-sectional components of $\boldsymbol{e}$ are the engineering shear strains ($2\varepsilon_{\alpha3}=\boldsymbol{e}\cdot\boldsymbol{d}_\alpha$), and the axial component of $\boldsymbol{e}$ is the axial extension ($\varepsilon_{33}=\boldsymbol{e}\cdot\boldsymbol{t}$).

For elastic rods, the strain energy function $\mathcal{U}$ is assumed to be a quadratic function of the arguments $\{\boldsymbol{e},\boldsymbol{\kappa}\}$, in the form

$$\rho_0\mathcal{U}(\boldsymbol{e},\boldsymbol{\kappa})=\frac{1}{2}\boldsymbol{e}\cdot\boldsymbol{A}\cdot\boldsymbol{e}+\boldsymbol{e}\cdot\boldsymbol{B}\cdot\boldsymbol{\kappa}+\frac{1}{2}\boldsymbol{\kappa}\cdot\boldsymbol{C}\cdot\boldsymbol{\kappa}. \tag{6}$$

Here, ρ_0 is the mass density per unit length of $\mathcal{C}_0$, while $\boldsymbol{A},\boldsymbol{B},\boldsymbol{C}$ are second order constitutive tensors, defined on the reference configuration. The structure of constitutive tensors for composite rods is (Bîrsan et al., 2012)

$$\begin{aligned}&\boldsymbol{A}=A_1\boldsymbol{d}_1\otimes\boldsymbol{d}_1+A_2\boldsymbol{d}_2\otimes\boldsymbol{d}_2+A_3\boldsymbol{t}\otimes\boldsymbol{t}+A_{12}(\boldsymbol{d}_1\otimes\boldsymbol{d}_2+\boldsymbol{d}_2\otimes\boldsymbol{d}_1),\\ &\boldsymbol{B}=B_{13}\boldsymbol{d}_1\otimes\boldsymbol{t}+B_{31}\boldsymbol{t}\otimes\boldsymbol{d}_1+B_{23}\boldsymbol{d}_2\otimes\boldsymbol{t}+B_{32}\boldsymbol{t}\otimes\boldsymbol{d}_2,\\ &\boldsymbol{C}=C_1\boldsymbol{d}_1\otimes\boldsymbol{d}_1+C_2\boldsymbol{d}_2\otimes\boldsymbol{d}_2+C_3\boldsymbol{t}\otimes\boldsymbol{t}+C_{12}(\boldsymbol{d}_1\otimes\boldsymbol{d}_2+\boldsymbol{d}_2\otimes\boldsymbol{d}_1).\end{aligned} \tag{7}$$

The constitutive coefficients $A_i, C_i, A_{12}, C_{12}, B_{\alpha3}$ and $B_{3\alpha}$ describe the effective stiffness properties of thin rods. The following energy equation holds in the linear theory, for all motions (Zhilin, 2007; Bîrsan and Altenbach, 2011a)

$$\rho_0\dot{\mathcal{U}} = \boldsymbol{N}\cdot\dot{\boldsymbol{e}} + \boldsymbol{M}\cdot\dot{\boldsymbol{\kappa}}, \tag{8}$$

where $\boldsymbol{N}$ is the force vector field, $\boldsymbol{M}$ is the moment vector field, and a superposed dot denotes the time derivative. Thus, $\boldsymbol{e}$ is the conjugate variable to $\boldsymbol{N}$ and $\boldsymbol{\kappa}$ is the conjugate variable to M. Then, the constitutive equations for composite elastic rods are written as

$$\boldsymbol{N} = \frac{\partial(\rho_0\mathcal{U})}{\partial\boldsymbol{e}}, \quad \boldsymbol{M} = \frac{\partial(\rho_0\mathcal{U})}{\partial\boldsymbol{\kappa}}. \tag{9}$$

The equations of motion have the form

$$\begin{aligned}\boldsymbol{N}' + \rho_0\mathcal{F} &= \rho_0(\ddot{\boldsymbol{u}} + \boldsymbol{\Theta}_1\cdot\ddot{\boldsymbol{\psi}}), \quad \boldsymbol{M}' + \boldsymbol{t}\times\boldsymbol{N} + \rho_0\mathcal{L}\\ &= \rho_0(\ddot{\boldsymbol{u}}\cdot\boldsymbol{\Theta}_1 + \boldsymbol{\Theta}_2\cdot\ddot{\boldsymbol{\psi}}),\end{aligned} \tag{10}$$

where $\mathcal{F}$ and $\mathcal{L}$ are the external body force and moment per unit mass, while $\boldsymbol{\Theta}_\alpha(s)$ are the inertia tensors in the reference configuration. To write the boundary conditions, we denote the length of the rod by l and the two endpoints by $\bar{s}_1 = 0$ and $\bar{s}_2 = l$. We consider general boundary conditions of the mixed type

$$\begin{aligned}&\boldsymbol{u}(\bar{s}_\gamma) = \boldsymbol{u}^{(\gamma)} \quad \text{or} \quad \boldsymbol{N}(\bar{s}_\gamma) = \boldsymbol{N}^{(\gamma)}, \quad \text{for} \quad \gamma = 1,2,\\ &\boldsymbol{\psi}(\bar{s}_\gamma) = \boldsymbol{\psi}^{(\gamma)} \quad \text{or} \quad \boldsymbol{M}(\bar{s}_\gamma) = \boldsymbol{M}^{(\gamma)}, \quad \text{for} \quad \gamma = 1,2,\end{aligned} \tag{11}$$

where the values $\boldsymbol{u}^{(\gamma)}, \boldsymbol{\psi}^{(\gamma)}, \boldsymbol{N}^{(\gamma)}, \boldsymbol{M}^{(\gamma)}$ are prescribed.

The condition that the strain energy density defined by (6) and (7) is a positive-definite function of the strains $\{\boldsymbol{e}, \boldsymbol{\kappa}\}$ is equivalent to the following restrictions on the constitutive coefficients

$$\begin{aligned}&A_1 > 0, \quad A_1A_2 - (A_{12})^2 > 0, \quad A_3 > 0, \quad A_3C_1 - (B_{31})^2 > 0,\\ &\begin{vmatrix} A_1 & A_{12} & B_{13}\\ A_{12} & A_2 & B_{23}\\ B_{13} & B_{23} & C_3\end{vmatrix} > 0, \quad \begin{vmatrix} A_3 & B_{31} & B_{32}\\ B_{31} & C_1 & C_{12}\\ B_{32} & C_{12} & C_2\end{vmatrix} > 0.\end{aligned} \tag{12}$$

The relations (1), (6), (7), (9) and (10) are the basic equations of the linear theory for directed curves, which are applicable to curved composite rods. In what follows, in order to simplify these equations, we restrict our attention to the case of straight composite rods (without natural twisting). We can chose the Cartesian coordinate frame $Ox_1x_2x_3$ such that the reference curve $\mathcal{C}_0$ is situated on the axis Ox_3, between the limits $x_3 = 0, l$. The axis Ox_1 and Ox_2 are chosen along the direction of the vectors $\boldsymbol{d}_1$ and $\boldsymbol{d}_2$, which coincide with the principal axes of inertia of the cross-section. If we denote by Σ the domain occupied by the cross-section of the rod in the x_1Ox_2 plane, it follows that

$$\int_\Sigma \rho x_1\mathrm{d}x_1\mathrm{d}x_2 = \int_\Sigma \rho x_2\mathrm{d}x_1\mathrm{d}x_2 = 0, \quad \int_\Sigma \rho x_1x_2\mathrm{d}x_1\mathrm{d}x_2 = 0, \tag{13}$$

where ρ is the mass density in the three-dimensional rod. Let $\boldsymbol{e}_i$ be the unit vectors along the axes Ox_i $(i = 1,2,3)$. Then we have $\boldsymbol{d}_1 = \boldsymbol{e}_1$, $\boldsymbol{d}_2 = \boldsymbol{e}_2$, $\boldsymbol{d}_3 = \boldsymbol{e}_3 = \boldsymbol{t}$ and $s = x_3$. We designate the inertia moments of the cross-section by

$$I_1 = \langle\rho x_2^2\rangle, \quad I_2 = \langle\rho x_1^2\rangle, \tag{14}$$

where we use the notation $\langle f\rangle = \int_\Sigma f\mathrm{d}x_1\mathrm{d}x_2$ for any field f.

Let us write now the basic equations for composite straight rods in components forms. To distinguish between the extensional (axial), torsional, bending, and shear deformation, we decompose the vectors $\boldsymbol{u}, \boldsymbol{\psi}, \boldsymbol{N}, \boldsymbol{M}, \mathcal{F}$ and $\mathcal{L}$ by the axial direction $\boldsymbol{e}_3$ and the normal plane $(\boldsymbol{e}_1, \boldsymbol{e}_2)$:

$$\begin{aligned}&\boldsymbol{u} = u\boldsymbol{e}_3 + \boldsymbol{w}, \quad \boldsymbol{\psi} = \psi\boldsymbol{e}_3 + \boldsymbol{e}_3\times\boldsymbol{\vartheta},\\ &\boldsymbol{N} = F\boldsymbol{e}_3 + \boldsymbol{Q}, \quad \boldsymbol{M} = H\boldsymbol{e}_3 + \boldsymbol{e}_3\times\boldsymbol{L}, \quad \mathcal{F} = \mathcal{F}_a\boldsymbol{e}_3 + \mathcal{F}_n,\\ &\mathcal{L} = \mathcal{L}_a\boldsymbol{e}_3 + \mathcal{L}_n.\end{aligned} \tag{15}$$

The vectors $\boldsymbol{w}, \boldsymbol{\vartheta}, \boldsymbol{Q}, \boldsymbol{L}, \mathcal{F}_n$ and $\mathcal{L}_n$ are orthogonal to $\boldsymbol{e}_3$. Here $u$is the longitudinal displacement, $\boldsymbol{w} = w_\alpha\boldsymbol{e}_\alpha$ is the vector of transversal displacement, ψ is the torsion, $\boldsymbol{\vartheta}' = \vartheta'_\alpha\boldsymbol{e}_\alpha$ is the vector of bending deformation, F is the longitudinal force, $\boldsymbol{Q} = Q_\alpha\boldsymbol{e}_\alpha$ is the vector of transversal force, $H$is the torsion moment and $\boldsymbol{L} = L_\alpha\boldsymbol{e}_\alpha$ is the vector of bending moment. With the notations (15), the constitutive Eqs. (6)–(9) can be put in the component form

$$\begin{aligned}&Q_1 = A_1(w_1' - \vartheta_1) + A_{12}(w_2' - \vartheta_2) + B_{13}\psi',\\ &Q_2 = A_{12}(w_1' - \vartheta_1) + A_2(w_2' - \vartheta_2) + B_{23}\psi',\\ &F = A_3u' - B_{31}\vartheta_2' + B_{32}\vartheta_1', \quad H = C_3\psi' + B_{13}(w_1' - \vartheta_1) + B_{23}(w_2' - \vartheta_2),\\ &L_1 = C_2\vartheta_1' - C_{12}\vartheta_2' + B_{32}u', \quad L_2 = -C_{12}\vartheta_1' + C_1\vartheta_2' - B_{31}u'.\end{aligned} \tag{16}$$

In this paper we consider non-homogeneous rods which properties are independent of the axial coordinate x_3. Then, the constitutive coefficients $A_i, C_i, A_{12}, C_{12}, B_{\alpha3}$ and $B_{3\alpha}$ are constants, which describe the effective stiffness properties of composite rods. In order to characterize their mechanical behavior, we will express these constitutive coefficients in terms of the three-dimensional elasticities, for a large variety of composite rods.

3. Effective stiffness properties for non-homogeneous rods

The relations (16) shows that C_1 and C_2 represent the bending effective stiffness coefficients, C_3 characterizes the torsional rigidity, A_1 and A_2 are the shear effective stiffness coefficients, A_3 expresses the extensional effective stiffness, while $B_{\alpha3}, B_{3\alpha}, C_{12}, A_{12}$ are coupling coefficients. To determine the effective stiffness coefficients $A_i, C_i, A_{12}, C_{12}, B_{\alpha3}$ and $B_{3\alpha}$ we compare the solutions of some extension, bending and torsion problems for directed curves with the corresponding results obtained for three-dimensional rods, see e.g. Ieşan (2009). The comparison procedure is described in details in Bîrsan et al. (2012). The relationship between the fields defined in the direct approach and the three-dimensional fields is given by

$$\begin{aligned}&\rho_0w_\alpha = \langle\rho u_\alpha^*\rangle, \quad \rho_0u = \langle\rho u_3^*\rangle, \quad \rho_0 = \langle\rho\rangle,\\ &\vartheta_1 = -\frac{\langle\rho x_1u_3^*\rangle}{I_2}, \quad \vartheta_2 = -\frac{\langle\rho x_2u_3^*\rangle}{I_1}, \quad \psi = \frac{\langle\rho(x_1u_2^* - x_2u_1^*)\rangle}{I_1 + I_2},\\ &Q_\alpha = \langle t_{3\alpha}^*\rangle, \quad F = \langle t_{33}^*\rangle, \quad L_\alpha = -\langle x_\alpha t_{33}^*\rangle, \quad H = \langle x_1t_{32}^* - x_2t_{31}^*\rangle,\end{aligned} \tag{17}$$

where u_i^* and t_{ij}^* are the components of the displacement vector $\boldsymbol{u}^*$ and the Cauchy tensor $\boldsymbol{T}^*$ for three-dimensional rods.

Remark. The relations of identification for displacements and rotations of the type (17) are obtained in the theory of directed curves (Zhilin, 2007) by imposing the condition that the linear momentum and the moment of momentum (per unit length of $\mathcal{C}_0$) are equal to the corresponding linear momentum and moment of momentum of the three-dimensional rod. This is the reason why the displacement and rotation fields are mass weighted in the comparison with three-dimensional fields (17). This is particularly significant for composite rods, when the difference between the mass densities of the constituents can be considerably, see the examples treated in the next sections.

It should be mentioned that the relations (17) are not the only possibility to relate the displacement and rotation fields with the three-dimensional quantities. Indeed, in view of the relations (2), (3) and (13), we see that the three-dimensional displacement $\boldsymbol{u}^* = \boldsymbol{R}^* - \boldsymbol{r}^*$ satisfies

$$\frac{\langle\rho x_\alpha\boldsymbol{u}^*\rangle}{\langle\rho x_\alpha^2\rangle} = \frac{\langle\boldsymbol{u}_{,\alpha}^*\rangle}{\mathrm{Area}(\Sigma)}, \quad \alpha = 1,2. \tag{18}$$

In the theory of Cosserat rods see Rubin (2000) the identification relations of the type (17) are expressed with the help of the integrals $\langle\boldsymbol{u}_{,\alpha}^*\rangle$. Note that the value of the shear correction coefficient depends generally on the specifications like (17), cf. (Rubin, 2003).

We assume that the three-dimensional rod is made of an isotropic and non-homogeneous material, characterized by the mass density $\rho = \rho(x_1, x_2)$ and the Lamé's moduli $\lambda = \lambda(x_1, x_2)$ and $\mu = \mu(x_1, x_2)$. We mention that the three-dimensional solutions used for comparison are exact solutions of the Saint–Venant relaxed problem for the bending, torsion and extension of solid composite cylinders, presented in Ieşan (1987, 2009). Even if the deformation of cross-sections is not taken into account for directed curves, the displacement fields in the two approaches should coincide, when calculated in the average sense (17).

It is known that the solution of the extension-bending-torsion problem for three-dimensional rods is expressed in terms of the solution to some auxiliary plane strain boundary-value problems, see e.g. Ieşan (2009), Sections 3.3 and 3.4. More precisely, let us denote by $\mathcal{D}^{(1)}$, $\mathcal{D}^{(2)}$ and $\mathcal{D}^{(3)}$ the plane strain problems defined on the domain Σ by

$$\mathcal{D}^{(\gamma)}: \begin{cases} \left[\lambda u_{\rho,\rho}\delta_{\alpha\beta} + \mu(u_{\alpha,\beta} + u_{\beta,\alpha})\right]_{,\beta} = -(\lambda x_\gamma)_{,\alpha} & \text{in} \quad \Sigma, \\ \left[\lambda u_{\rho,\rho}\delta_{\alpha\beta} + \mu(u_{\alpha,\beta} + u_{\beta,\alpha})\right] n_\beta = -\lambda x_\gamma n_\alpha & \text{on} \quad \partial\Sigma, \end{cases} \quad (\gamma = 1,2)$$

$$\mathcal{D}^{(3)}: \begin{cases} \left[\lambda u_{\rho,\rho}\delta_{\alpha\beta} + \mu(u_{\alpha,\beta} + u_{\beta,\alpha})\right]_{,\beta} = -\lambda_{,\alpha} & \text{in} \quad \Sigma, \\ \left[\lambda u_{\rho,\rho}\delta_{\alpha\beta} + \mu(u_{\alpha,\beta} + u_{\beta,\alpha})\right] n_\beta = -\lambda n_\alpha & \text{on} \quad \partial\Sigma, \end{cases} \quad (19)$$

where $\delta_{\alpha\beta}$ is the Kronecker symbol. The solution of the problem $\mathcal{D}^{(k)}$ will be denoted by $u_\alpha^{(k)}(x_1, x_2)$, for every $k = 1, 2, 3$. On the other hand, the torsion function $\varphi(x_1, x_2)$ is the solution of the Neumann type boundary-value problem

$$\begin{aligned} &\left(\mu\varphi_{,\alpha}\right)_{,\alpha} = \mu_{,1}x_2 - \mu_{,2}x_1 \quad \text{in} \quad \Sigma, \\ &\frac{\partial\varphi}{\partial n} = x_2 n_1 - x_1 n_2 \quad \text{on} \quad \partial\Sigma, \end{aligned} \quad (20)$$

where the vector $\boldsymbol{n} = n_\alpha \boldsymbol{e}_\alpha$ is the outward unit normal to $\partial\Sigma$.

Taking into account the relations (17), we find that the solutions of the extension-bending-torsion problems coincide in the two approaches (direct and three-dimensional) provided the effective stiffness coefficients are given by Bîrsan et al. (2012)

$$\begin{aligned} &A_3 = \left\langle (\lambda + 2\mu) + \lambda u_{\gamma,\gamma}^{(3)} \right\rangle, \quad B_{\alpha 3} = 0, \quad B_{31} = \left\langle x_2(\lambda + 2\mu + \lambda u_{\gamma,\gamma}^{(3)}) \right\rangle, \\ &B_{32} = -\left\langle x_1(\lambda + 2\mu + \lambda u_{\gamma,\gamma}^{(3)}) \right\rangle, \quad C_1 = \left\langle x_2\left[(\lambda + 2\mu)x_2 + \lambda u_{\gamma,\gamma}^{(2)}\right] \right\rangle, \\ &C_2 = \left\langle x_1\left[(\lambda + 2\mu)x_1 + \lambda u_{\gamma,\gamma}^{(1)}\right] \right\rangle, \quad C_{12} = -\left\langle x_1\left[(\lambda + 2\mu)x_2 + \lambda u_{\gamma,\gamma}^{(2)}\right] \right\rangle, \\ &C_3 = \left\langle \mu[x_1(x_1 + \varphi_{,2}) + x_2(x_2 - \varphi_{,1})] \right\rangle. \end{aligned} \quad (21)$$

To determine the shear effective stiffness coefficients A_1 and A_2 we consider the shear vibrations of rectangular rods in the two approaches (direct and three-dimensional). By identifying the lowest natural frequencies, we obtain the expressions (Bîrsan et al., 2012)

$$\begin{aligned} &A_\alpha = \kappa\langle\mu\rangle \frac{\langle\rho x_\alpha^2\rangle \text{Area}(\Sigma)}{\langle\rho\rangle\langle x_\alpha^2\rangle}, \\ &A_{12} = 0, \quad \alpha = 1,2 (\text{not summed}), \end{aligned} \quad (22)$$

where the factor $\kappa = \frac{\pi^2}{12}$ is similar to the shear correction factor introduced first by Timoshenko in the theory of beams (see Timoshenko, 1921, where the value $\kappa = \frac{5}{6}$ is proposed).

Remark. We mention that the relations (22) have been derived by approximation of more detailed formulas obtained for rectangular beams. We present next the exact formulas for shear stiffness in the case of non-homogeneous rectangular rods. Let $\Sigma = \{(x_1, x_2) | x_1 \in (-\frac{a}{2}, \frac{a}{2}), x_2 \in (-\frac{b}{2}, \frac{b}{2})\}$ be the cross-section domain and $\rho(x_1, x_2)$ be the mass density such that $\rho(x_1, x_2) = \rho(x_1, -x_2)$. Then, the shear stiffness coefficient A_2 is expressed by Bîrsan et al. (2012)

$$A_2 = \kappa\langle\mu\rangle \frac{\langle\rho x_2^2\rangle \text{ Area}(\Sigma)}{\langle\rho(x_1, \beta)\rangle\langle x_2^2\rangle}, \quad (23)$$

where $\beta(x_1, x_2) \in (-\frac{b}{2}, \frac{b}{2})$ is an intermediate point such that

$$\langle\rho(x_1, \beta)\rangle = -\frac{\pi}{b}\int_{-\frac{a}{2}}^{\frac{a}{2}}\int_{-\frac{b}{2}}^{\frac{b}{2}} \left(\cos\frac{\pi x_2}{b}\right)^{-1} \left(\int_{-\frac{b}{2}}^{x_2} \rho(x_1, \xi)\sin\frac{\pi\xi}{b} \mathrm{d}\xi\right) \mathrm{d}x_2 \mathrm{d}x_1. \quad (24)$$

A similar formula holds for A_1. In most cases, we can use the approximation $\langle\rho(x_1, \beta)\rangle \simeq \langle\rho(x_1, x_2)\rangle$ and the exact relation (23) reduces to the simplified expression (22).

4. Effective stiffness properties for composite beams

In this section we generalize the results of the previous section to the case of composite rods. More precisely, we consider that the composite beam is made of n different non-homogeneous materials. We consider separately the cases when the n constituent materials are isotropic or orthotropic.

Let the rod-like body be denoted by $\mathcal{B} = \{(x_1, x_2, x_3) | (x_1, x_2) \in \Sigma, x_3 \in (0, l)\}$. For composite beams, the cross-section Σ is partitioned into $n$sub-domains $S_1, \ldots, S_n$ with $S_k \cap S_l = \emptyset$, for $k \neq l$. As shown in Fig. 2(a), the generic cross-section Σ may include a number of m'layers' $S_1, \ldots, S_m$ (with $0 \leqslant m \leqslant n$) and an arbitrary number of 'inclusions' $S_{m+1}, \ldots, S_n$. Then the beam $\mathcal{B}$ is decomposed into $n$regions $\mathcal{B}_k = \{(x_1, x_2, x_3) | (x_1, x_2) \in S_k, x_3 \in (0, l)\}$, such that each domain $\mathcal{B}_k$ is occupied by a different non-homogeneous material characterized by the mass density and the Lamé's moduli

$$\begin{aligned} &\rho = \rho^{(k)}(x_1, x_2), \quad \lambda = \lambda^{(k)}(x_1, x_2), \\ &\mu = \mu^{(k)}(x_1, x_2) \quad \text{in} \quad S_k \quad (1 \leqslant k \leqslant n). \end{aligned} \quad (25)$$

We consider that the bodies $\mathcal{B}_k$ are welded together and there is no separation of material during deformation. The displacement vector field and the stress vector field are continuous in passing from one material to another.

We designate by $\mathcal{C}_k$ the boundary curve of the domain S_k which does not belong to the cross-section boundary $\partial\Sigma$, i.e. $\mathcal{C}_k = \partial S_k \setminus \partial\Sigma$. We assume that the curves $\mathcal{C}_k$ $(k = 1, \ldots, n)$ are not self-intersecting, like in Fig. 2(a). For any boundary curve $\mathcal{C}_k$ which separates the domains S_l and S_r such that $l < r$ (here either $l = k$ or $r = k$), we denote by $\boldsymbol{n} = n_\alpha \boldsymbol{e}_\alpha$ the unit normal to $\mathcal{C}_k$ pointing toward S_r (Fig. 2(b)) and introduce the notation

$$[f]_-^+ = f^{(r)} - f^{(l)} \quad \text{on} \quad \mathcal{C}_k, \quad \text{for any field } f, \quad (26)$$

where $f^{(r)}$ designates the field f calculated in S_r.

In the case of composite beams, the plane strain boundary-value problems of the type (19), (20) will have a more complicated form, because we have to adjoin the continuity conditions on the

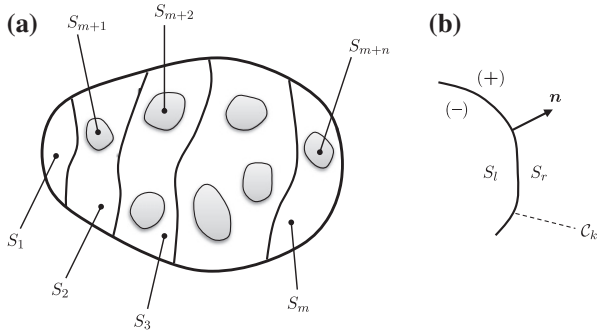

Fig. 2. (a) The cross-section of a general composite beams; (b) The separation curve between the domains S_l and S_r.

curves of separation $\mathcal{C}_k$ between the n materials. Let us denote by $\mathcal{P}^{(1)}$, $\mathcal{P}^{(2)}$ and $\mathcal{P}^{(3)}$ the following plane strain problems defined on the domain Σ

$$\mathcal{P}^{(\gamma)}:\begin{cases} t_{\beta\alpha,\beta}=-(\lambda x_\gamma)_{,\alpha} \text{ in } S_k \ (k=1,\dots,n),\\ t_{\beta\alpha}n_\beta=-\lambda x_\gamma n_\alpha \text{ on } \partial\Sigma,\\ [u_\alpha]^+_-=0,\ n_\beta\left[t_{\beta\alpha}+\lambda x_\gamma\delta_{\alpha\beta}\right]^+_-=0 \text{ on } \mathcal{C}_k \ (k=1,\dots,n),\end{cases} \quad (\gamma=1,2)$$

$$\mathcal{P}^{(3)}:\begin{cases} t_{\beta\alpha,\beta}=-\lambda_{,\alpha} \quad \text{in} \quad S_k \quad (k=1,\dots,n),\\ t_{\beta\alpha}n_\beta=-\lambda n_\alpha \quad \text{on} \quad \partial\Sigma,\\ [u_\alpha]^+_-=0, \quad n_\beta\left[t_{\beta\alpha}+\lambda\delta_{\alpha\beta}\right]^+_-=0 \quad \text{on} \quad \mathcal{C}_k \quad (k=1,\dots,n),\end{cases} \tag{27}$$

where we denote by $t_{\alpha\beta}=\lambda u_{\rho,\rho}\delta_{\alpha\beta}+\mu(u_{\alpha,\beta}+u_{\beta,\alpha})$. The solution of the problem $\mathcal{P}^{(s)}$ will be denoted by $u^{(s)}_\alpha(x_1,x_2)$, $s=1,2,3$. For the torsion function $\varphi(x_1,x_2)$ we have to solve the boundary-value problem of the Neumann type

$$\begin{cases} \left(\mu\varphi_{,\alpha}\right)_{,\alpha}=\mu_{,1}x_2-\mu_{,2}x_1 \quad \text{in} \quad S_k \quad (k=1,\dots,n),\\ \frac{\partial\varphi}{\partial n}=x_2n_1-x_1n_2 \quad \text{on} \quad \partial\Sigma,\\ [\varphi]^+_-=0, \quad \left[\mu\left(\frac{\partial\varphi}{\partial n}-x_2n_1+x_1n_2\right)\right]^+_-=0 \quad \text{on} \quad \mathcal{C}_k \quad (k=1,\dots,n).\end{cases} \tag{28}$$

The existence of solutions to the plane strain boundary-value problems (27), (28) can be shown in the same manner as in Ieşan (2009) Section 3.6.1, where the case $n=2$ is considered.

Extending the procedure described in Section 5 of Bîrsan et al. (2012) to the case of n materials, we find that the effective stiffness coefficients for composite rods are expressed by

$$\begin{aligned} A_3&=\sum_{k=1}^n\int_{S_k}\left(\lambda^{(k)}+2\mu^{(k)}+\lambda^{(k)}u^{(3)}_{\gamma,\gamma}\right)\mathrm{d}x_1\mathrm{d}x_2, \quad B_{13}=B_{23}=0,\\ B_{31}&=\sum_{k=1}^n\int_{S_k}x_2\left(\lambda^{(k)}+2\mu^{(k)}+\lambda^{(k)}u^{(3)}_{\gamma,\gamma}\right)\mathrm{d}x_1\mathrm{d}x_2,\\ B_{32}&=-\sum_{k=1}^n\int_{S_k}x_1\left(\lambda^{(k)}+2\mu^{(k)}+\lambda^{(k)}u^{(3)}_{\gamma,\gamma}\right)\mathrm{d}x_1\mathrm{d}x_2,\\ C_1&=\sum_{k=1}^n\int_{S_k}x_2\left[(\lambda^{(k)}+2\mu^{(k)})x_2+\lambda^{(k)}u^{(2)}_{\gamma,\gamma}\right]\mathrm{d}x_1\mathrm{d}x_2,\\ C_2&=\sum_{k=1}^n\int_{S_k}x_1\left[(\lambda^{(k)}+2\mu^{(k)})x_1+\lambda^{(k)}u^{(1)}_{\gamma,\gamma}\right]\mathrm{d}x_1\mathrm{d}x_2,\\ C_{12}&=-\sum_{k=1}^n\int_{S_k}x_1\left[(\lambda^{(k)}+2\mu^{(k)})x_2+\lambda^{(k)}u^{(2)}_{\gamma,\gamma}\right]\mathrm{d}x_1\mathrm{d}x_2,\\ C_3&=\sum_{k=1}^n\int_{S_k}\mu^{(k)}\left[x_1(x_1+\varphi_{,2})+x_2(x_2-\varphi_{,1})\right]\mathrm{d}x_1\mathrm{d}x_2.\end{aligned} \tag{29}$$

The relations (22) for effective shear stiffness in the case of composite beams become

$$A_\alpha=\frac{\kappa\mathrm{Area}(\Sigma)}{\langle x^2_\alpha\rangle}\left(\sum_{k=1}^n\int_{S_k}\mu^{(k)}\mathrm{d}x_1\mathrm{d}x_2\right)\left(\sum_{k=1}^n\int_{S_k}\rho^{(k)}x^2_\alpha\mathrm{d}x_1\mathrm{d}x_2\right)\left(\sum_{k=1}^n\int_{S_k}\rho^{(k)}\mathrm{d}x_1\mathrm{d}x_2\right)^{-1}. \tag{30}$$

where $\kappa=\frac{\pi^2}{12}$ is the shear correction factor.

The relations (29) and (30) give the exact values for the effective stiffness properties of beams made of $n$different non-homogeneous materials. These formulas apply to very general situations. However, it is not easy to use them in some practical cases, since it is difficult to obtain the solutions to the plane strain boundary-value problems (27), (28).

In the remaining of this paper we present some important instances where we can apply the above formulas, including sandwich beams with foam core, sandwich circular columns and functionally graded beams.

4.1. Composite beams with constant Poisson ratio

Let us present an important case when the plane strain boundary-value problems (27), (28) are easily solvable, and the relations for the effective stiffness coefficients (29), (30) admit a significant simplification. This is the case of composite beams with constant Poisson ratio, the same constant for all material constituents. Within the classical three-dimensional elasticity theory, the case of non-homogeneous materials with constant Poisson ratio has been studied in details, see e.g. Lomakin (1976).

For the non-homogeneous material occupying the domain $\mathcal{B}_k$ we denote by $E^{(k)}(x_1,x_2)$ the Young modulus and by $\nu^{(k)}(x_1,x_2)$ the Poisson ratio. In this section we assume that

$$\nu^{(k)}(x_1,x_2)=\nu \text{ (constant)}, \quad \text{for } k=1,\dots,n. \tag{31}$$

In this situation, the plane strain boundary-value problems $\mathcal{P}^{(s)}$ given by (27) admit simple solutions $u^{(s)}_\alpha$, $s=1,2,3$. It is easy to prove that

$$\begin{aligned} &u^{(1)}_1=-\frac{1}{2}\nu(x_1^2-x_2^2), \quad u^{(1)}_2=-\nu x_1x_2,\\ &u^{(2)}_1=-\nu x_1x_2, \quad u^{(2)}_2=\frac{1}{2}\nu(x_1^2-x_2^2), \quad u^{(3)}_1=-\nu x_1, \quad u^{(3)}_2=-\nu x_2\end{aligned} \tag{32}$$

satisfy all the equations and conditions in (27). Inserting the functions (32) into the formulas (29), we obtain in this case the following effective stiffness coefficients

$$\begin{aligned} &A_3=\sum_{k=1}^n\int_{S_k}E^{(k)}\mathrm{d}x_1\mathrm{d}x_2, \quad B_{31}=\sum_{k=1}^n\int_{S_k}x_2E^{(k)}\mathrm{d}x_1\mathrm{d}x_2, \quad B_{\alpha3}=0,\\ &B_{32}=-\sum_{k=1}^n\int_{S_k}x_1E^{(k)}\mathrm{d}x_1\mathrm{d}x_2, \quad C_1=\sum_{k=1}^n\int_{S_k}x_2^2E^{(k)}\mathrm{d}x_1\mathrm{d}x_2,\\ &C_2=\sum_{k=1}^n\int_{S_k}x_1^2E^{(k)}\mathrm{d}x_1\mathrm{d}x_2, \quad C_{12}=-\sum_{k=1}^n\int_{S_k}x_1x_2E^{(k)}\mathrm{d}x_1\mathrm{d}x_2.\end{aligned} \tag{33}$$

The relations (33) have a more classical form but we should emphasize that, from a mathematical point of view, they are valid only in the case when the Poisson ratios of the $n$different materials are equal. The expressions for the torsional rigidity C_3 and shear effective stiffness A_1,A_2 remain the same as in $(29)_8$ and (30), independent of any assumption on the Poisson ratio.

In the next sections we will employ the above relations to evaluate the effective stiffness properties of various sandwich beam structures.

5. Sandwich beams with foam core

In this section we consider sandwich beams with rectangular cross-section. The *faces* of the beam are assumed to be of equal thicknesses and made of the same material, while the *core* is made of a different material (foam). In typical sandwich structures, the faces are usually thin and stiff, but the core is weak and lightweight. These types of structures are widely used (for example in aviation or automotive applications) because they provide a high bending stiffness coupled with light weight. For a detailed description and analysis of sandwich structures with foam core, we refer to the classical books of Allen (1969); Zenkert (1997); Gibson and Ashby (1997).

Let us denote by c and t_f the thicknesses of the core and the faces, respectively, $a=c+2t_f$ is the total thickness of the beam,

b designates the width of the beam, d is the distance between the middle axes of the faces, see Fig. 3(a). Assume that the materials are homogeneous and isotropic and denote by ρ_c, E_c, G_c the mass density, Young's modulus, shear modulus for the core, while ρ_f, E_f, G_f designate the corresponding quantities for the faces.

The stiffness properties which are of special interest for this sandwich beam are: the torsional rigidity C_3, the bending effective stiffness C_1 about the Ox_1 axis, and the shear effective stiffness A_2 in the x_2 direction. Let us evaluate these stiffness properties using the general formulas from Section 4, and compare our results with previously known values from the literature.

5.1. Torsional rigidity

In order to calculate the torsional rigidity C_3 using the Eq. $(29)_8$ we need to determine first the torsion function $\varphi(x_1,x_2)$ by solving the boundary-value problem (28) written for our configuration. Taking into account the geometry of the cross-section (Fig. 3(a)) in this case we have

$$\Sigma=\left\{(x_1,x_2)|x_1\in\left(-\frac{b}{2},\frac{b}{2}\right),x_2\in\left(-\frac{a}{2},\frac{a}{2}\right)\right\},\ S_1=\left\{(x_1,x_2)|x_1\in\left(-\frac{b}{2},\frac{b}{2}\right),x_2\in\left(-\frac{a}{2},-\frac{c}{2}\right)\right\},$$
$$S_2=\left\{(x_1,x_2)|x_1\in\left(-\frac{b}{2},\frac{b}{2}\right),x_2\in\left(\frac{c}{2},\frac{a}{2}\right)\right\},\ S_3=\left\{(x_1,x_2)|x_1\in\left(-\frac{b}{2},\frac{b}{2}\right),x_2\in\left(-\frac{c}{2},\frac{c}{2}\right)\right\}.$$

Then, the boundary-value problem (28) becomes

$$\begin{cases}\Delta\varphi=0 \quad \text{in} \quad S_1\cup S_2\cup S_3,\\ \frac{\partial\varphi}{\partial n}=x_2n_1-x_1n_2 \quad \text{for} \quad x_1=\pm\frac{b}{2} \quad \text{or} \quad x_2=\pm\frac{a}{2},\\ [\varphi]^+_-=0, \quad \left[G\left(\frac{\partial\varphi}{\partial n}-x_2n_1+x_1n_2\right)\right]^+_-=0 \quad \text{for} \quad x_2=\pm\frac{c}{2},\end{cases} \tag{34}$$

where $\Delta=\frac{\partial^2}{\partial x_1^2}+\frac{\partial^2}{\partial x_2^2}$ is the Laplace operator. We search for a solution of (34) in the form of a series

$$\varphi(x_1,x_2)=x_1x_2+\sum_{n=0}^{\infty}f_n(x_2)\sin(mx_1), \quad \text{with} \quad m=\frac{(2n+1)\pi}{b}, \tag{35}$$

where the function $f_n(x_2)$ is expressed by

$$f_n(x_2)=A_n^{(k)}\sinh(mx_2)+B_n^{(k)}\cosh(mx_2) \quad \text{in} \quad S_k \quad (k=1,2,3).$$

The constants $A_n^{(k)}$ and $B_n^{(k)}$ are then determined by imposing that the conditions $(34)_{2,3,4}$ are satisfied. Finally, from the relation $(29)_8$ we obtain the torsional rigidity

$$C_3=\frac{b^3}{3}\left[(cG_c+2t_fG_f)-\frac{192\cdot b}{\pi^5}\sum_{n=0}^{\infty}\frac{C_{(n)}}{(2n+1)^5}\right], \tag{36}$$

where we denote by

$$C_{(n)}=\frac{G_c(G_c\cosh(mt_f)\tanh\frac{mc}{2}+G_f\sinh(mt_f))+2G_f(G_c-G_f)(1-\cosh(mt_f))\tanh\frac{mc}{2}}{G_c\cosh(mt_f)+G_f\sinh(mt_f)\tanh\frac{mc}{2}}. \tag{37}$$

The series from (36) converges very rapidly, so that we can obtain good approximations of C_3 by keeping only few terms.

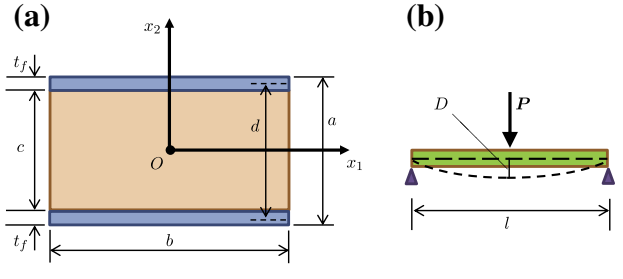

Fig. 3. (a) Cross-section of a sandwich beam; (b) Three-point bending of a beam.

Remark.

1. In the case of a 'monolithic' beam, i.e. if we take $G_c=G_f$ in the formula (36), then we obtain the well-known expression for the torsional rigidity of rectangular beams, see e.g. Timoshenko and Goodier (1951), p. 278:
$$C_3=G\frac{b^3a}{3}\left[1-\frac{192\cdot b}{\pi^5a}\sum_{n=0}^{\infty}\frac{1}{(2n+1)^5}\tanh\frac{(2n+1)\pi a}{2b}\right]. \tag{38}$$
2. Let us consider the case when the core shear modulus is much smaller than the shear modulus of the faces: $G_c\ll G_f$. This assumption is reasonable in most practical situations. If we neglect the ratio $\frac{G_c}{G_f}\simeq 0$, then the relation (37) simplifies to $C_{(n)}\simeq 2G_f\tanh(mt_f/2)$. Then the formula (36) for the torsional rigidity shows that in this case the beam acts like two faces twisting independently of each other.

Let us compare the torsional rigidity found in (36) with the torsional rigidity for sandwich beams given in Zenkert (1997), Section 3.12:

$$\widetilde{C}_3=G_f\frac{b}{3}\left[a^3+\left(\frac{G_c}{G_f}-1\right)c^3\right]. \tag{39}$$

The formula (39) is valid only for *wide* beams (sandwich panels), i.e. when b is much larger than the thickness of the beam a (Zenkert, 1997; Seide, 1956). We remark that if we take $G_c=G_f$ in the relation (39) (the 'monolithic' case), then we obtain $\widetilde{C}_3=Gba^3/3$ which is the *limiting value* as $b\gg a$ for the torsional rigidity of rectangular beams. We will compare the values (36) and (39) graphically, in terms of the ratio between the thickness and the width of the beam. Let us denote by δ,ε and r the following ratios

$$\delta=\frac{2t_f}{b}, \quad \varepsilon=\frac{c}{b}, \quad r=\frac{G_c}{G_f}. \tag{40}$$

Then the values for the torsional rigidity given by (36) and (39) can be written as

$$C_3=G_f\frac{b^4}{3}f(\delta,\varepsilon), \quad \widetilde{C}_3=G_f\frac{b^4}{3}g(\delta,\varepsilon), \tag{41}$$

where we have introduced the non-dimensional functions

$$g(\delta,\varepsilon)=(\delta+\varepsilon)^3+(r-1)\varepsilon^3,\ f(\delta,\varepsilon)=(\delta+\varepsilon r)-\frac{192}{\pi^5}\sum_{n=0}^{\infty}\frac{1}{(2n+1)^5}$$
$$\times\frac{r[\tanh(k\delta)+r\tanh(k\varepsilon)]+2(1-r)\tanh(k\delta)\tanh(k\varepsilon)\tanh(k\delta/2)}{r+\tanh(k\delta)\tanh(k\varepsilon)}, \tag{42}$$

with $k=\frac{(2n+1)\pi}{2}$ and $r=\frac{G_c}{G_f}$. We want to compare the functions f and g for small values of δ and ε, since $\delta+\varepsilon=a/b$ and the range of applicability of the formula (39) is restricted to wide beams.

Let us take an example of a sandwich beam for which $G_c/G_f=0.1$ and $2t_f/c=0.2$. In this case we have $r=0.1$ and $\delta=0.2\,\varepsilon$, and the graphics of f and g as functions of ε are depicted in Fig. 4. From the graphic we can see that the values of f and g are very close for $\varepsilon<0.25$, i.e. when the thickness-to-width ratio satisfies $a/b<0.3$.

Next, we compare the functions f and g in the more general case when the ratios $\delta=\frac{2t_f}{b}$ and $\varepsilon=\frac{c}{b}$ vary independently, and the materials are such that $r=\frac{G_c}{G_f}=0.4$. We plot the difference function $(g-f)(\delta,\varepsilon)$ and obtain the surface in Fig. 5(a). The level curves of this surface are represented in Fig. 5(b), which shows that the difference between f and g is very small for $\delta+\varepsilon<0.3$, i.e. when the ratio $a/b<0.3$.

As a conclusion of the above analysis, we deduce that the simple formula (39) for torsional rigidity can be used for wide sandwich

beam satisfying $\frac{a}{b} < 0.3$, but if the thickness-to-width ratio $\frac{a}{b}$ is bigger than 0.3, the exact formula (36) should be employed.

5.2. Effective bending stiffness and shear stiffness

To obtain simple expressions for the effective bending stiffness coefficient C_1 we assume in this section that the Poisson ratios of the two materials are equal: $\nu_f = \nu_c$. Then, we can employ the formula $(33)_5$ to evaluate the effective bending stiffness C_1. Taking into account the geometry of the cross-section (Fig. 3(a)) from $(33)_5$ we obtain

$$C_1 = E_f \frac{bt_f d^2}{2} + E_f \frac{bt_f^3}{6} + E_c \frac{bc^3}{12}. \tag{43}$$

This relation for the effective bending stiffness for sandwich beams coincides with the classical result presented in Allen (1969), Zenkert (1997), Gibson and Ashby (1997).

If we employ the exact formula (23) for effective shear stiffness, in our case we find

$$A_2 = \kappa \frac{12b}{a^2} \frac{cG_c + 2t_f G_f}{c\rho_c + 2t_f\rho_f + c(\rho_f - \rho_c)F(\frac{\pi c}{2a})} \left(\rho_f \frac{t_f d^2}{2} + \rho_f \frac{t_f^3}{6} + \rho_c \frac{c^3}{12}\right), \tag{44}$$

where the function $F(\cdot)$ is defined on the interval $(-\frac{\pi}{2}, \frac{\pi}{2})$ by

$$F(x) = \frac{\cos x}{x} \ln\left(\frac{1+\sin x}{\cos x}\right) \quad \text{for} \quad x \neq 0, \quad F(0) = 1. \tag{45}$$

We observe that $F(-x) = F(x)$ and $\lim_{x\to 0} F(x) = 1$, so the function is continuous. Also, we have $\lim_{x\nearrow\frac{\pi}{2}} F(x) = 0$. The graphic of the function $F(x)$ on the interval $(-\frac{\pi}{2}, \frac{\pi}{2})$ is depicted in Fig. 6.

On the other hand, the classical expression of the effective shear stiffness A_2 for sandwich beams is

$$\widetilde{A}_2 = \frac{bd^2}{c} G_c, \tag{46}$$

which in the case of *thin faces* (i.e. $t_f \ll c$) admits the approximation (Allen, 1969; Gibson and Ashby, 1997)

$$\widetilde{A}_2 = bcG_c. \tag{47}$$

Let us present a simplified (approximate) version of the exact formula (44) for the effective shear stiffness A_2 in the case of thin faces, and find the correlation with the classical result (47). In this case, the value of $\frac{c}{a}$ is very close to 1 and since $\lim_{x\nearrow\frac{\pi}{2}} F(x) = 0$, the term $F(\frac{\pi c}{2a})$ is negligible in (44). We consider that the ratio $\epsilon \equiv \frac{t_f}{c}$ is small (since faces are thin), and we develop the expression in the right-hand side of (44) as a power series of ϵ. If we neglect all the terms of order $\mathcal{O}(\epsilon^2)$ and higher, we get the approximate formula

$$A_2 = \kappa b\left(cG_c + 2t_f G_f + 4t_f G_c \frac{\rho_f - \rho_c}{\rho_c}\right). \tag{48}$$

Moreover, if we neglect also the terms of first order $\mathcal{O}(\epsilon)$ (applicable for *very thin faces*), then we obtain the relation

$$A_2 = \kappa bcG_c, \tag{49}$$

which corresponds to the classical value (47) with the shear correction factor κ included.

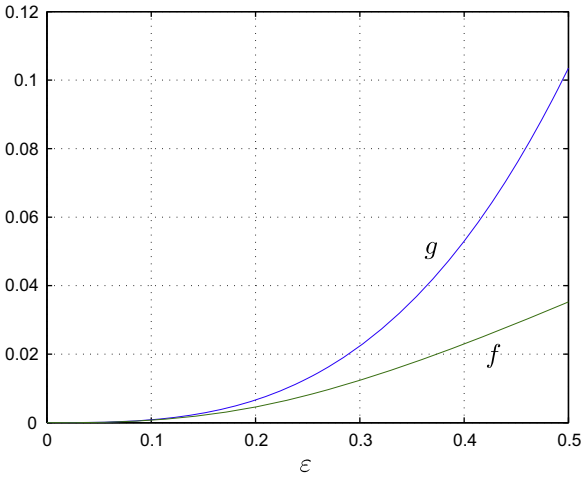

Fig. 4. The graphics of f and g as functions of the ratio $\varepsilon = c/b$.

5.3. Three-point bending of sandwich beams

To validate the values of the effective stiffness properties obtained above, we analyze a three-point bending problem and compare our theoretical results with experimental data. Let us consider sandwich beams (with polyester or epoxy faces and foam core) subjected to a central load P, with simply supported ends, as depicted in Fig. 3(b). The analytical solution of this three-point bending problem is not difficult to calculate using the direct approach of rods. We find that the maximum deflection D of the beam is given by the well-known formula

$$D = \frac{Pl}{4}\left(\frac{1}{A_2} + \frac{l^2}{12C_1}\right), \tag{50}$$

where the effective bending stiffness C_1 and the effective shear stiffness A_2 are given by (43) and (44). On the other hand, according to the classical approach (Zenkert, 1997; Gibson and Ashby, 1997) the maximum deflection is evaluated from the relation

$$\widetilde{D} = \frac{Pl}{4}\left(\frac{1}{\widetilde{A}_2} + \frac{l^2}{12C_1}\right), \tag{51}$$

where $\widetilde{A}_2$ is given by (46). The difference resides in the effective shear stiffness A_2. Let us compare the predictions stated in (50) and (51) with some experimental results.

The three-point bending tests were performed on the Strength of Materials Laboratory from the Faculty of Mechanical Engineering at Lublin University of Technology. A 25 kN MTS static and dynamic testing machine type 858 Table Top System was used for bending tests, using 2.5 kN load cell range. Fig. 7(a) shows the positioning of the specimen, while Fig. 7(b) presents the specimens used in the experiments Marsavina et al. (2008); Marsavina et al. (2010). Tests were performed at room temperature and with a 5 mm/min test speed, according to ASTM C393-00 Standard Test Methods for Flexural Properties of Sandwich Constructions (American Society of Testing and Materials, 2000). The load and the displacement were recorded during tests.

Two types of sandwich beams with foam core have been tested in three-point bending: beams with polyester faces, and beams with epoxy faces. A 200 kg/m^3 density rigid polyurethane foam was used in the experimental program for the core material. The polyurethane foams were impregnated with polyester and epoxy resins, which form the faces (skins of the sandwich). Polyurethane foams are widely used as cores in sandwich composites, for packing and cushioning. They are made of interconnected networks of solid struts or plates which form the edges and the faces of the closed cells.

To calculate the Young's modulus E_c and the shear modulus G_c for foams with closed cells we use the relations (Gibson and Ashby, 1997), p. 197:

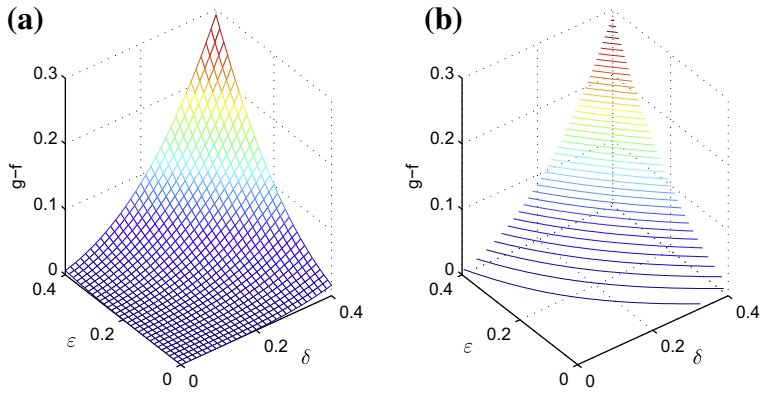

Fig. 5. The difference function $g - f$ in terms of (δ, ε).

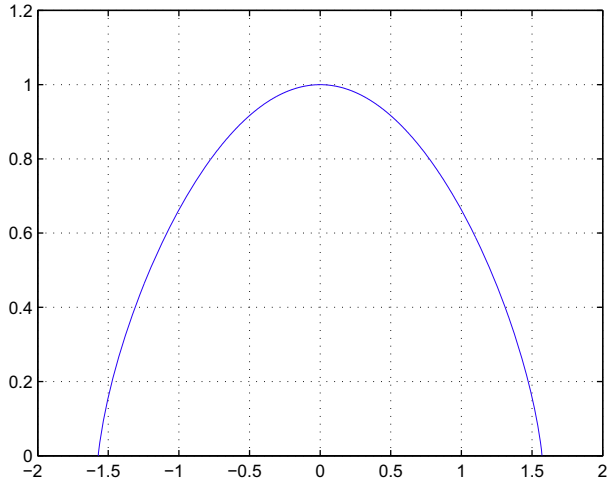

Fig. 6. The graphic of function $F(x)$ on the interval $(-\frac{\pi}{2}, \frac{\pi}{2})$.

$$\frac{E_c}{E_s} = \phi^2 \left(\frac{\rho_c}{\rho_s}\right)^2 + (1-\phi)\frac{\rho_c}{\rho_s},$$
$$\frac{G_c}{E_s} = \frac{3}{8}\left[\phi^2 \left(\frac{\rho_c}{\rho_s}\right)^2 + (1-\phi)\frac{\rho_c}{\rho_s}\right], \tag{52}$$

where E_s and ρ_s are the Young's modulus and mass density of the solid material which constitutes the foam, while ϕ is the volume fraction of solid material contained in the cell edges (and $1-\phi$ represents the fraction of solid material contained in the faces of closed cells, see Gibson and Ashby (1997), p. 40 for details). For rigid polyurethane foams we have $\phi = 0.8$ according to Gibson and Ashby (1997), Reitz et al. (1984), so the material parameters are $\rho_s = 1170\ \text{Kg/m}^3$, $E_s = 1600$ MPa.

The span length of the tested sandwich beams is $l = 90$ mm, and the width $b = 12.2$ mm. Other geometrical and material parameters of the sandwich beams are listed in the Table 1, cf. (Linul et al., 2011). In Fig. 8 we represent graphically the dependence of the load P versus the maximum deflection D, for the sandwich beam with epoxy faces and polyurethane foam core. We have plotted three different theoretical predictions: the classical solution (51), (46), the exact analytical solution (50), (44), and the approximate analytical solution (50) with the effective shear stiffness given by (48). We have also depicted the results of experimental measurements in the linear elastic regime. The graphic shows that the exact analytical solution, obtained on the basis of formula (44) for the effective shear stiffness, can describe better the experimental data, in comparison with the classical results. We observe that the approximate analytical solution (48) is very close to the exact analytical solution (44).

The experimental tests were performed up to failure, but in this analysis we considered only the linear elastic region.

In the case of sandwich beams with polyester faces and polyurethane foam core, the dependence of the maximum deflection D on the load P is depicted in Fig. 9. We see from the graphic that the exact analytical solution provides a better prediction of experimental measurements, also for polyester–polyurethane sandwich beams. We observe that the exact analytical solution is intermediate between the classical and the approximate analytical solutions, and the difference between them is very small.

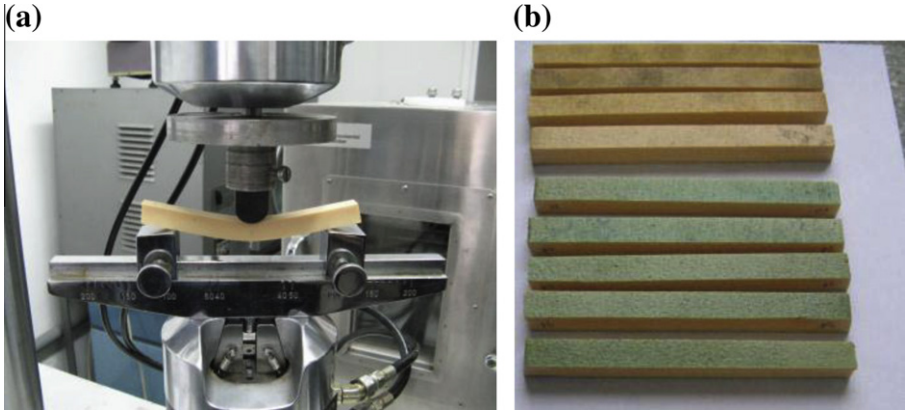

Fig. 7. (a) MTS 25 kN testing machine; (b) specimens of sandwich beams used in experiments.

Table 1
Geometrical and material parameters of the sandwich beam.

Face	Core	t_f [mm]	c [mm]	E_f [MPa]	E_c [MPa]	G_f [MPa]	G_c [MPa]	$\rho_f \left[\frac{\text{Kg}}{\text{m}^3}\right]$	$\rho_c \left[\frac{\text{Kg}}{\text{m}^3}\right]$
Polyester	Foam	0.1	12	4000	74.8	1400	28.05	1200	200
Epoxy	Foam	0.17	12.03	3400	74.8	1353.5	28.05	1060	200

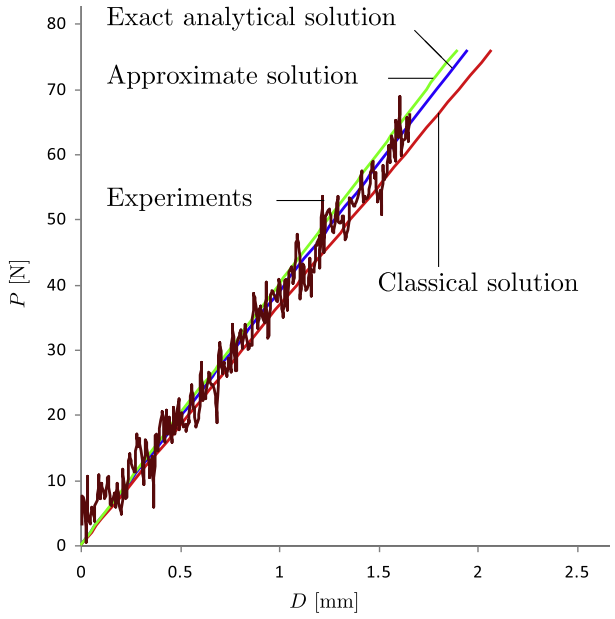

Fig. 8. The load P versus deflection D for a sandwich beam with epoxy faces and polyurethane foam core: comparison between analytical solutions and experimental results.

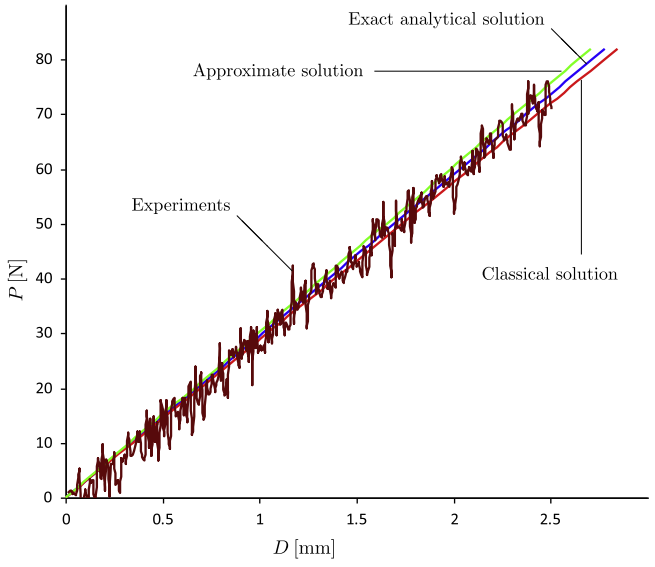

Fig. 9. The load P versus deflection D for a sandwich beam with polyester faces and polyurethane foam core: comparison between analytical solutions and experimental results.

6. Sandwich beams with dissimilar faces

In this section we consider non-symmetrical sandwich beams with faces of different thicknesses and materials. We denote by t_1, ρ_1, E_1, and G_1 the thickness, density, Young's modulus, and shear modulus of the upper face, and by t_2, ρ_2, E_2, and G_2 the corresponding quantities for the lower face. As in the preceding section, we designate by c the core's thickness, $d = c + \frac{t_1+t_2}{2}$ is the distance between the middle axis of the faces, and e is the distance between Ox_1 and the middle axis of the lower face, see Fig. 10(a).

The position of the axes Ox_1 and Ox_2 is determined by the conditions (13). Then the distance e is given by

$$e = \frac{c\rho_c(c+t_2)/2 + dt_1\rho_1}{c\rho_c + t_1\rho_1 + t_2\rho_2}. \tag{53}$$

We assume that the materials have the same Poisson ratios. In this case, the effective stiffness coefficients can be calculated using the expressions (33). Thus, for the effective bending stiffness we obtain the formula

$$C_1 = b\left[\frac{E_c c^3}{12} + \frac{E_1 t_1^3}{12} + \frac{E_2 t_2^3}{12} + E_c c\left(\frac{c+t_2}{2} - e\right)^2 + E_1 t_1 (d-e)^2 + E_2 t_2 e^2\right]. \tag{54}$$

Let us calculate the effective shear stiffness A_2. On the basis of the exact formula (23), we obtain for A_2 the following expression

$$A_2 = \kappa \frac{ab}{z_0^3 - z_3^3} \times \frac{(t_1G_1 + t_2G_2 + cG_c)\left[\rho_1(z_0^3 - z_1^3) + \rho_c(z_1^3 - z_2^3) + \rho_2(z_2^3 - z_3^3)\right]}{(t_1\rho_1 + t_2\rho_2 + c\rho_c) + (\rho_1 - \rho_c)z_1 F(\frac{\pi z_1}{a}) + (\rho_c - \rho_2)z_2 F(\frac{\pi z_2}{a})}, \tag{55}$$

where the function F is defined in (45), and $z_0, \ldots, z_3$ are given by

$$\begin{aligned} z_0 &= \frac{\frac{t_1}{2}t_1\rho_1 + (t_1 + \frac{c}{2})c\rho_c + (t_1 + c + \frac{t_2}{2})t_2\rho_2}{t_1\rho_1 + t_2\rho_2 + c\rho_c}, \\ z_1 &= \frac{-\frac{t_1}{2}t_1\rho_1 + \frac{c}{2}c\rho_c + (c + \frac{t_2}{2})t_2\rho_2}{t_1\rho_1 + t_2\rho_2 + c\rho_c}, \\ z_2 &= \frac{-(c + \frac{t_1}{2})t_1\rho_1 - \frac{c}{2}c\rho_c + \frac{t_2}{2}t_2\rho_2}{t_1\rho_1 + t_2\rho_2 + c\rho_c}, \\ z_3 &= -\frac{(\frac{t_1}{2} + c + t_2)t_1\rho_1 + (\frac{c}{2} + t_2)c\rho_c + \frac{t_2}{2}t_2\rho_2}{t_1\rho_1 + t_2\rho_2 + c\rho_c}. \end{aligned} \tag{56}$$

On the other hand, if we employ the approximate formula (30) to evaluate A_2, we get

$$A_2 = \kappa b(t_1G_1 + t_2G_2 + cG_c) \cdot K(t_1\rho_1, t_2\rho_2, c\rho_c), \tag{57}$$

where we denote by $K(\cdot,\cdot,\cdot)$ the expression

$$K(r_1, r_2, r_c) = \frac{(r_1+r_2+r_c)(r_1t_1^2 + r_2t_2^2 + r_ct_c^2) + 3\left[4r_1r_2d^2 + r_1r_c(t_1+t_c)^2 + r_2r_c(t_2+t_c)^2\right]}{a^2(r_1+r_2+r_c)^2 + 3[r_c(t_1-t_2) - r_1(t_2+t_c) + r_2(t_1+t_c)]^2}. \tag{58}$$

In the *thin faces approximation* (i.e. when $t_1, t_2 \ll c$) we neglect the second order terms in the small parameters $(\frac{t_1}{c}, \frac{t_2}{c})$ and hence, the expression (57) simplifies to

$$A_2 = \kappa b\left[(t_1G_1 + t_2G_2 + cG_c) + 2t_1G_c\left(\frac{\rho_1}{\rho_c} - 1\right) + 2t_2G_c\left(\frac{\rho_2}{\rho_c} - 1\right)\right]. \tag{59}$$

If the faces are very thin, then we can also neglect the first order terms in $(\frac{t_1}{c}, \frac{t_2}{c})$ and from (59) we find the approximate formula $A_2 = \kappa bcG_c$ which is in agreement with the classical approximate result, see e.g. Gibson and Ashby (1997), p. 350.

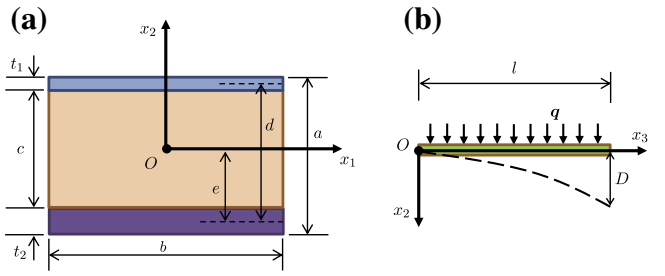

Fig. 10. (a) Cross-section of a sandwich beam with dissimilar faces; (b) Cantilever beam with uniform distributed load q.

The remaining effective stiffness coefficients are calculated without difficulty by applying the general relations (30) and (33). We obtain

$$A_3 = b(t_1E_1 + t_2E_2 + cE_c), \quad C_2 = \frac{b^3}{12}(t_1E_1 + t_2E_2 + cE_c), \quad C_{12} = 0,$$
$$B_{31} = -b\left[t_1E_1(e-d) + t_2E_2e + cE_c\left(e - \frac{t_2+t_c}{2}\right)\right], \quad B_{32} = B_{\alpha 3} = 0. \tag{60}$$

We notice that the coupling coefficient B_{31} is nonzero, due to the non-symmetry of the beam in the x_2 direction.

Remark. In the case when the Poisson ratios of the materials are not equal, it is difficult to compute the effective bending stiffness C_α using the relations (29), since we have to solve first the boundary-value problem (27). On the other hand, the effective shear stiffness A_α keep the same form even in this case, by virtue of (23) or (30). We notice that the general formulas (30) and (33) can also be used to calculate the effective stiffness coefficients for multilayered beams with an arbitrary number of layers.

7. Functionally graded sandwich columns

Other types of sandwich structures with important applications are the square columns and the circular columns, cf. (Gibson and Ashby, 1997) Section 9.2, as shown in Fig. 11(a).

For these types of composite beams we can compute the effective stiffness coefficients by applying the general relations (29) and (30). Assume that the cross-section Σ of the beam has the geometry presented in Fig. 11(b), and denote by ν_c, E_c, ρ_c, G_c the material parameters for the core, and by ν_f, E_f, ρ_f, G_f the material parameters for the face.

Let us consider circular sandwich columns made of functionally graded materials and determine its effective stiffness properties. The generic cross-section of the beam is described in Fig. 11(b). Assume that the core material has the mass density ρ_c and the Lamé moduli λ_c and μ_c, expressed by exponential law distributions through radial direction

$$\rho_c = \rho_0 \exp(-\sigma r), \quad \lambda_c = \lambda_0 \exp(-\sigma r), \quad \mu_c = \mu_0 \exp(-\sigma r), \tag{61}$$

where $r = \sqrt{x_1^2 + x_2^2}$ is the radial distance and σ is a constant exponent. This kind of cylindrical inhomogeneity has been intensively studied in classical elasticity, see e.g. Lomakin (1976). We employ the obvious notations $\nu_0 = \frac{\lambda_0}{2(\lambda_0+\mu_0)}$ and $E_0 = \frac{\mu_0(3\lambda_0+2\mu_0)}{\lambda_0+\mu_0}$.

The face of the sandwich column is made of a functionally graded material characterized by the following parameters

$$\rho_f = \rho(r), \quad E_f = E(r), \quad \nu_f = \nu_0 \quad (\text{constant}), \tag{62}$$

where $\rho(r)$ and $E(r)$ are arbitrary given functions of r.

Using the relations (61) and (62) in our particular geometry, we obtain from the general formulas (33) the effective extensional stiffness and bending stiffness coefficients

$$A_3 = 2\pi \int_{R_1}^{R_2} rE(r)\mathrm{d}r + \frac{2\pi}{\sigma^2}E_0\left[1 - (1+\sigma R_1)e^{-\sigma R_1}\right],$$
$$C_1 = C_2 = \pi \int_{R_1}^{R_2} r^3E(r)\mathrm{d}r + \frac{\pi}{\sigma^4}E_0\left[6 - (6 + 6\sigma R_1 + 3\sigma^2R_1^2 + \sigma^3R_1^3)e^{-\sigma R_1}\right], \tag{63}$$

and $B_{3\alpha} = 0$, $C_{12} = 0$. Since the boundary-value problem (28) admits in this case the solution $\varphi = 0$, we can easily apply the formula $(29)_8$ and find the torsional rigidity in the form

$$C_3 = \frac{\pi}{1+\nu_0}\int_{R_1}^{R_2} r^3E(r)\mathrm{d}r + \frac{2\pi}{\sigma^4}\mu_0\left[6 - (6 + 6\sigma R_1 + 3\sigma^2R_1^2 + \sigma^3R_1^3)e^{-\sigma R_1}\right]. \tag{64}$$

On the basis of relations (30), (61) and (62), we get the following expression for the effective shear stiffness

$$A_1 = A_2 = \frac{2\pi\kappa}{R_2^2}\cdot\frac{\frac{1}{1+\nu_0}\int_{R_1}^{R_2} rE(r)\mathrm{d}r + \frac{2}{\sigma^2}\mu_0\left[1-(1+\sigma R_1)e^{-\sigma R_1}\right]}{\int_{R_1}^{R_2} r\rho(r)\mathrm{d}r + \frac{1}{\sigma^2}\rho_0[1-(1+\sigma R_1)e^{-\sigma R_1}]} \times\left\{\int_{R_1}^{R_2} r^3\rho(r)\mathrm{d}r + \frac{1}{\sigma^4}\rho_0\left[6-(6+6\sigma R_1+3\sigma^2R_1^2+\sigma^3R_1^3)e^{-\sigma R_1}\right]\right\}. \tag{65}$$

To conclude, all the effective stiffness coefficients for this type of FGM sandwich column have been calculated.

Let us verify the values of the effective stiffness coefficients (63)–(65) by comparison between the analytical solutions and numerical results obtained with ABAQUS, for some basic elastostatic problems: bending of cantilever FGM beam, torsion and extension of FGM circular sandwich column.

For our numerical example, we consider a circular cylindrical beam as described in Fig. 11, with length $l = 20$ cm and radii $R_1 = 1.25$ cm, $R_2 = 1.5$ cm. The core is made of a functionally graded material having the elastic properties given by the exponential distribution law (61) with $E_0 = 343$ GPa, $\nu_0 = 0.3$, $\rho_0 = 3880$ kg/m^3, which corresponds to alumina (Ootao, 2011). For the exponent σ we take 5 different values: $\sigma \in \{25, 50, 75, 100, 150\}$. The dependence of the Young modulus $E_c = E_0\exp(-\sigma r)$ on the radial distance r is depicted in Fig. 12.

We assume that the exterior layer (skin) of the sandwich column is made of a homogeneous material (aluminum alloy) characterized by $E_f = 70$ GPa and $\rho_f = 2688$ kg/m^3.

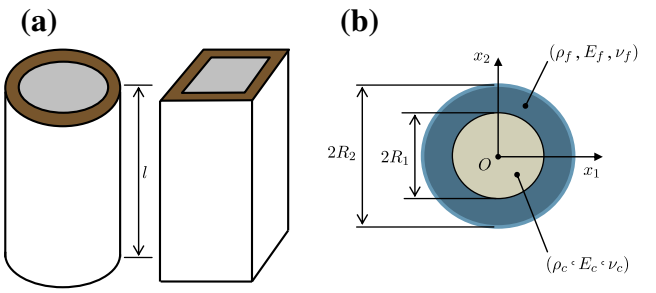

Fig. 11. (a) Circular and rectangular sandwich columns; (b) Cross-section of a circular sandwich column.

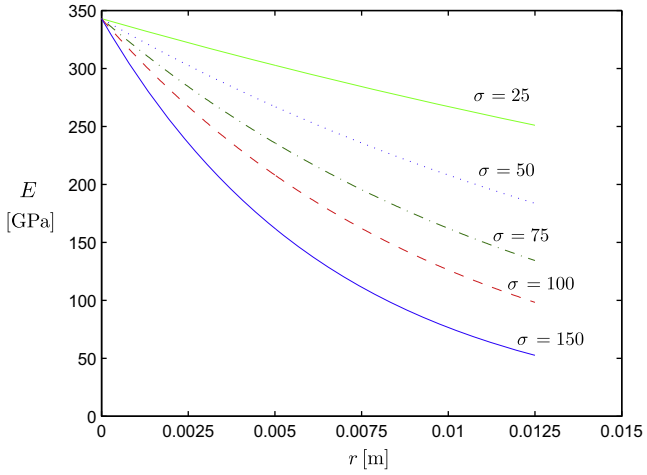

Fig. 12. The distribution of Young modulus E in the core, for different values of the exponent σ.

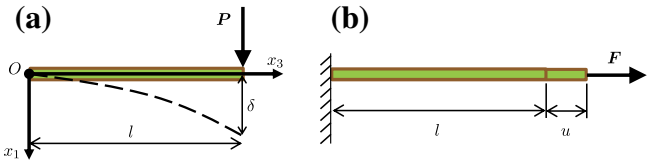

Fig. 13. (a) Cantilever beam with concentrated end force P; (b) Extension of FGM sandwich column.

Table 2
Comparison of results for FGM cantilever beam with concentrated end load.

σ	25	50	75	100	150
δ_{exact} [mm]	0.2527	0.3045	0.3618	0.4237	0.5551
δ_{FEM} [mm]	0.2523	0.3034	0.3600	0.4209	0.5502
Error Δ [%]	−0.1719	−0.3532	−0.5012	−0.6658	−0.8962

In the finite element analysis with ABAQUS we will use elements of cylindrical type, and 3D stresses. The shape of elements is hexagonal. The functionally graded structure of the core is described by dividing the domain into 64 cylindrical layers with constant material parameters which satisfy the exponential law (61) stepwise.

7.1. Bending of cantilever FGM beam by end loads

Consider a cantilever beam subject to a concentrated end force $P = 616$ N acting in the x_1 direction, see Fig. 13(a). For the maximum deflection δ, the analytical solution predicts the following value

$$\delta_{\text{exact}} = Pl\left(\frac{1}{A_1} + \frac{l^2}{3C_2}\right), \tag{66}$$

where A_1 and C_2 are effective stiffness coefficients given by $(63)_2$ and (65). On the other hand, let δ_{FEM} denote the maximum deflection computed by the finite element analysis. The comparison between the theoretical and numerical results is presented in Table 2 and Fig. 14(a), where we denote by $\Delta = \frac{\delta_{\text{FEM}} - \delta_{\text{exact}}}{\min(\delta_{\text{FEM}}, \delta_{\text{exact}})}$ the relative error. We remark a very good agreement of the two approaches.

7.2. Torsion of FGM clamped sandwich column

Consider the circular sandwich column described above, subjected to torsion by the torque (twisting moment) $M = 0.467$ kN m acting at one end of the beam. The other end is clamped.

Denote by ψ the angle of twist at the loaded end of the beam. From the analytical solution we obtain the value $\psi_{\text{exact}} = \frac{Ml}{C_3}$, where the torsional rigidity C_3 is determined by (64).

In order to compare the beam-like solution ψ_{exact} with the numerical solution obtained by the finite element analysis, we calculate the angle of twist ψ_{FEM} in terms of the three-dimensional displacements by means of the formula $(17)_6$. The comparison between the theoretical and numerical values for the angle of twist is presented in Table 3, for different values of the exponent σ.

7.3. Extension of FGM sandwich column

Let us consider the extension of the circular FGM sandwich column by a given axial force F acting on its end edge. The other end of the beam is clamped, see Fig. 13(b). Denote by $u_{\text{exact}} = \frac{Fl}{A_3}$ the axial displacement at the loaded end, as predicted theoretically, where the extensional stiffness A_3 is determined by $(63)_1$.

For numerical calculations, we decompose the resultant force F as a uniformly distributed load $p = 100$ MPa over the end edge. If we designate by $(u_3^*)_{\text{FEM}}$ the three-dimensional axial displacement computed by the finite element analysis, then in virtue of relations $(17)_{2,3}$ the corresponding beam-like axial displacement is calculated from the formula $u_{\text{FEM}} = \frac{\langle \rho (u_3^*)_{\text{FEM}} \rangle}{\langle \rho \rangle}$. From Table 4 and

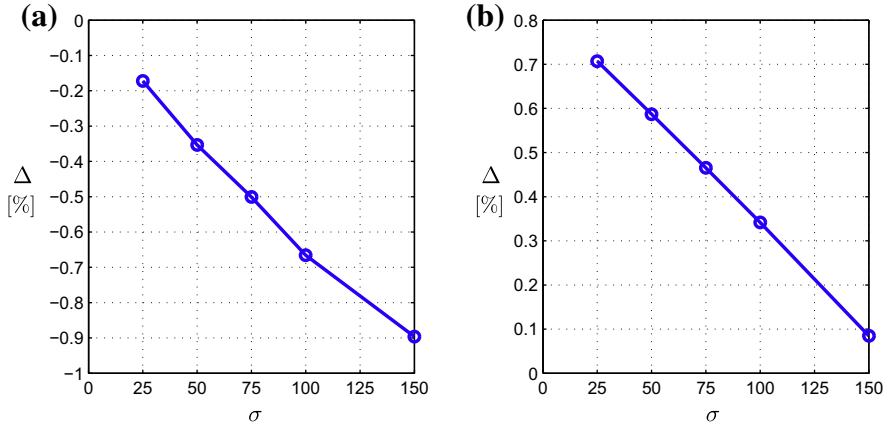

Fig. 14. The relative error Δ in terms of the exponent σ, for: (a) maximum deflection of a FGM cantilever beam; (b) axial displacement of a FGM sandwich column under extension.

Table 3
Analytical and numerical results for torsion of circular FGM sandwich column.

σ	25	50	75	100	150
ψ_{exact} [rad]	0.0185	0.0223	0.0265	0.0310	0.0406
ψ_{FEM} [rad]	0.0193	0.0233	0.0276	0.0323	0.0428
Error Δ [%]	4.4676	4.4847	4.3323	4.0513	5.3453

Table 4
Comparison of axial displacements obtained analytically and numerically for extension of FGM sandwich column.

σ	25	50	75	100	150
u_{exact} [mm]	0.0929	0.1110	0.1314	0.1542	0.2059
u_{FEM} [mm]	0.09354	0.1117	0.1321	0.1547	0.2060
Error Δ [%]	0.7073	0.587	0.4654	0.3417	0.0846

Fig. 14(b) we observe that the theoretical and numerical results u_{exact} and u_{FEM} are in very good agreement.

8. Conclusions

In this paper we have determined the effective stiffness properties of various composite beams, in order to characterize their mechanical behavior. The general formulas for the effective stiffness coefficients of composite beams made of several non-homogeneous isotropic materials are given by the relations (29) and (30). From these formulas we find by particularization the expressions of the effective bending stiffness, shear stiffness, extensional stiffness, and torsional rigidity, for some composite beams of interest: sandwich beams with foam core, sandwich beams with dissimilar faces, and functionally graded columns. Thus, for piecewise homogeneous sandwich beams we have obtained the torsional rigidity (36), the effective bending stiffness (43), and shear stiffness (44). These values have been compared with classical theoretical results in Sections 5.1, 5.2, and with experimental measurements for three-point bending in Section 5.3. The effective stiffness properties for sandwich beams with dissimilar faces have been presented in Section 6.

For circular sandwich columns made of functionally graded materials with exponential distribution law we have found the expressions (63)–(65) for the effective stiffness coefficients. Using these values, we have deduced the analytical beam-like solutions of some bending, torsion and extension problems, and compared them with numerical results in Sections 7.1, 7.2, 7.3.

The good agreement between the theoretical, experimental, and numerical results for the mechanical problems studied above represent a validation of our analytical formulas for the effective stiffness properties of sandwich composite beams.

Acknowledgements

The authors acknowledge funding from the E.U. FP7 Programme FP7-REGPOT-2009-1 under grant agreement No. 245479, and from the Polish Ministry of Science and Higher Education, Grant No. 1471-1/7, PR UE/2010/7.

References

Allen, H.G., 1969. Analysis and Design of Structural Sandwich Panels. Pergamon Press, Oxford.
American Society of Testing and Materials, 2000. ASTM Standard Test method for flexural properties of sandwich constructions (C393-00). ASTM International, West Conshohocken, Pennsylvania.
Antman, S.S., 1972. The theory of rods. In: S. Flugge (Ed.), Hanbuch der Physik, C Truesdell (Ed.), vol. VIa/2 , Springer-Verlag, Berlin, pp. 641–703.
Antman, S.S., 1995. Nonlinear problems of elasticity. Applied Mathemaical Sciences, 107. Springer-Verlag, Berlin.
Bîrsan, M., Altenbach, H., 2011a. On the theory of porous elastic rods. Int. J. Solids Struct. 48, 910–924.
Bîrsan, M., Altenbach, H., 2011b. Theory of thin thermoelastic rods made of porous materials. Arch. Appl. Mech. 81, 1365–1391.
Bîrsan, M., Altenbach, H., Sadowski, T., Eremeyev, V.A., Pietras, D., 2012. Deformation analysis of functionally graded beams by the direct approach. Composites Part B 43, 1315–1328.
Gibson, L.J., Ashby, M.F., 1997. Cellular Solids: Structure and Properties, Cambridge Solid State Science Series, second ed. Cambridge University Press, Cambridge.
Green, A.E., Naghdi, P.M., 1979. On thermal effects in the theory of rods. Int. J. Solids Struct. 15, 829–853.
Green, A.E., Naghdi, P.M., Wenner, M.L., 1979. On the theory of rods, I: derivations from the three-dimensional equations, II: developments by direct approach. Proc. R. Soc. London A337 (451–483), 485–507.
Ieşan, D., 1987. Saint-Venant' s problem. Lecture Notes in Mathematics, 1279. Springer-Verlag, Berlin, Heidelberg, New York.
Ieşan, D., 2009. Classical and Generalized Models of Elastic Rods. Chapman & Hall/CRC Press, Boca Raton, London, New York.
Linul, E., Marsavina, L., Cernescu, A., 2011. Assessment of sandwich beams using failure-mode maps. In: Proceedings of the 16th International Conference on Composite Structures, Porto, Portugal.
Lomakin, V.A., 1976. Theory of Nonhomogeneous Elastic Bodies. MGU, Moscow (in Russian).
Lurie, A.I., 2005. Theory of Elasticity. Springer, Berlin.
Marsavina, L., Sadowski, T., Constantinescu, D.M., Negru, R., 2008. Failure of polyurethane foams under different loading conditions. Key Eng. Mater. 385–387, 205–208.
Marsavina, L., Sadowski, T., Knec, M., Negru, R., 2010. Non-linear behaviour of foams under static and impact three point bending. Int. J. Non-Linear Mech. 45, 969–975.
Ootao, Y., 2011. Transient thermoelastic analysis for a multilayered thick strip with piecewise exponential nonhomogeneity. Composites Part B 42, 973–981.
Postek, E., Sadowski, T., 2011. Assessing the influence of porosity in the deformation of metal–ceramic composites. Compos. Interfaces 18, 57–76.
Reitz, D.W., Schuetz, M.A., Glicksman, L.R., 1984. A basic study of aging of foam insulation. J. Cell. Plast. 20, 104–113.
Rubin, M.B., 2000. Cosserat Theories: Shells, Rods, and Points. Kluwer Academic Publishers, Dordrecht.
Rubin, M.B., 2003. On the quest for the best Timoshenko shear coefficient. ASME J. Appl. Mech. 70, 154–157.
Sadowski, T., Hardy, S.J., Postek, E.W., 2005. Prediction of the mechanical response of polycrystalline ceramics containing metallic intergranular layers under uniaxial tension. Comput. Mater. Sci. 34, 46–63.
Sadowski, T., Hardy, S., Postek, E., 2006. A new model for the time-dependent behaviour of polycrystalline ceramic materials with metallic inter-granular layers under tension. Mater. Sci. Eng. A 424, 230–238.
Seide, P., 1956. On the torsion of rectangular sandwich plates. J. Appl. Mech. 23, 191–194.
Simo, J.C., 1985. A finite strain beam formulation, The three-dimensional dynamic problem, Part I. Comput. Methods Appl. Mech. Eng. 49, 55–70.
Timoshenko, S.P., 1921. On the correction for shear of the differential equation for transverse vibrations of prismatic beams. Philos. Mag. 41, 744–746.
Timoshenko, S., Goodier, J.N., 1951. Theory of Elasticity. McGraw-Hill, New York.
Zenkert, D., 1995. An Introduction to Sandwich Construction. Chameleon, London.
Zenkert, D., 1997. The Handook of Sandwich Construction. Engineering Materials Advisory Services Ltd. Publishing.
Zhilin, P.A., 2006. Nonlinear theory of thin rods. In: Indeitsev, D.A., Ivanova, E.A., Krivtsov, A.M. (Eds.), Advanced Problems in Mechanics, Institute for Problems Mechanical Engineering, vol. 2. R.A.S. Publ., St. Petersburg, pp. 227–249.
Zhilin, P.A., 2007. Applied Mechanics – Theory of Thin Elastic Rods. Politekhn. Univ. Publ, St. Petersburg (in Russian).